MATERIALS CHEMISTRY FRONTIERS

RESEARCH ARTICLE

View Article Online
View Journal | View Issue

Cite this: *Mater. Chem. Front.*, 2025, **9**, 2362

Enhancing the stability and emission efficiency of circularly polarized luminescent materials for deep blue applications†

Si-Fan Lu,[ab] Meng-Na Jing,[a] Mian-He Xu,[a] Jian Lu,*[ac] Fa-Kun Zheng [abc] and Guo-Cong Guo*[ab]

Received 7th February 2025,
Accepted 2nd May 2025

DOI: 10.1039/d5qm00119f

rsc.li/frontiers-materials

Circularly polarized luminescent (CPL) materials are essential for advanced optoelectronics, especially wide-color-gamut OLED displays. Here, BINAP-based enantiomers were synthesized *via* one-step methylation, yielding deep blue emission (CIE_y < 0.08) with high thermal stability and antioxidative properties, thus addressing the challenges in designing blue-emitting CPL materials for efficient, stable, and commercializable applications.

Circularly polarized luminescent (CPL) materials have garnered significant attention in recent years for their unique ability to emit circularly polarized light, enabling promising applications in advanced optoelectronic devices, including 3D displays, OLEDs, optical data storage, and spintronic devices.[1,2] Notably, circularly polarized blue-emitting materials are especially important for developing wide-color-gamut displays and full-color CPL devices, as blue light serves as a foundational primary color in the RGB (red, green, blue) model.[3–5] Despite the increasing demand for CPL materials, the development of efficient and stable blue-emitting materials remains challenging, as blue light, with its higher energy, is prone to poor photostability, thermal stability, and oxidation resistance when compared to its green and red counterparts, while simultaneously achieving a high dissymmetry factor (g_{lum})—a critical parameter quantifying the degree of circular polarization—is particularly difficult due to the inherent trade-offs between luminescence efficiency and molecular design for chirality.[6–8]

Recent advances in blue-emitting circularly polarized luminescent (CPL) materials aim to address challenges like photostability, thermal stability, and oxidation resistance.[9,10] Strategies include using chiral ligands to enhance the dissymmetry factor (g_{lum}) and luminescence efficiency; however, balancing chirality and efficiency can be difficult.[11] Hybrid organic–inorganic systems improve stability and emission properties but may suffer from inconsistencies in structure and morphology.[12–14] Additionally, engineering conjugated polymeric systems and introducing bulky groups can enhance robustness and tune emission wavelengths, but these modifications can reduce molecular packing efficiency and complicate large-scale fabrication.[15,16]

In light of the aforementioned considerations, the prototypical axially chiral small molecule 2,2′-bis(diphenylphosphino)-1,1′-binaphthalene (BINAP) was employed to synthesize a pair of enantiomers *via* a one-step methylation reaction. The resulting methylated derivatives exhibit deep blue emission with a CIE coordinate *y* value below 0.08. Moreover, these compounds demonstrate exceptional thermal stability and antioxidative properties. These findings underscore the promising potential of these materials as commercially viable candidates for circularly polarized luminescence applications, particularly in wide-color-gamut OLED displays, and provide a robust theoretical framework to facilitate the commercialization of circularly polarized deep-blue-emitting materials.

These chiral enantiomers, **1A** (*R*-CH_3) and **1B** (*S*-CH_3), can be efficiently prepared in large quantities using literature-reported methods, with the unbonded lone pairs of electrons on the phosphorus atoms conferring nucleophilicity for *in situ* methylation reactions.[17,18] Their colourless, transparent, rod-like microcrystals suitable for X-ray single-crystal diffractions can be obtained by allowing the filtrate to evaporate slowly at room temperature. The phase and purity of the as-synthesized enantiomers were further determined through characterization techniques such as PXRD, ^{1}H NMR, FT-IR/Raman, and TG & DSC (Fig. S1–S5, ESI†). As shown in Fig. 1b, X-ray single-crystal

[a] *State Key Laboratory of Structural Chemistry, Fujian Institute of Research on the Structure of Matter, Chinese Academy of Sciences, Fuzhou, Fujian 350002, P. R. China. E-mail: lujian@fjirsm.ac.cn, gcguo@fjirsm.ac.cn*
[b] *University of Chinese Academy of Science, Beijing, 100049, P. R. China*
[c] *Fujian Science & Technology Innovation Laboratory for Optoelectronic Information of China, Fuzhou, Fujian 350108, P. R. China*

† Electronic supplementary information (ESI) available: The powder XRD patterns, ^{1}H NMR spectra, FT-IR patterns, Raman spectra, TG & DSC curves, UV-Vis spectra, and stability test results of **1A** and **1B**. CCDC 2418303 (**1A**) and 2414162 (**1B**). For ESI and crystallographic data in CIF or other electronic format see DOI: https://doi.org/10.1039/d5qm00119f

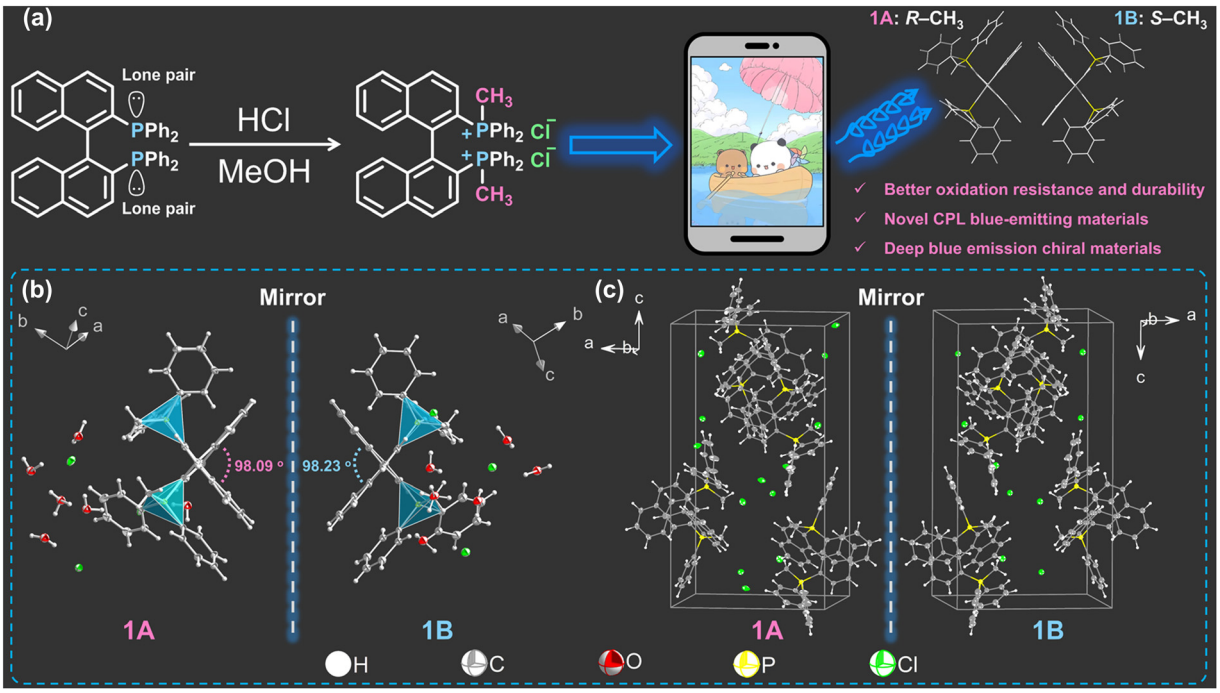

Fig. 1 (a) Strategies for the structure design of chiral organophosphorus compounds for application in display devices. (b) The minimal asymmetric unit structures of **1A** and **1B**. (c) The unit cell structures of **1A** and **1B**; all the crystalline water molecules are omitted for clarity.

diffraction data indicated that these crystalline chiral enantiomers belong to the orthorhombic crystal system with the chiral non-centrosymmetric space group $P2_12_12_1$. The dihedral angles of the naphthyl rings in **1A** and **1B** are 98.09° and 98.23°, respectively. The asymmetric unit contains one organophosphorus cation, in which the two phosphorus atoms have undergone an S_n2 reaction to form P^+–CH_3. Additionally, this unit includes three counter-anions Cl^-, one hydrated cation H_3O^+, and five crystalline water molecules. Furthermore, there are extensive weak interactions (including O–H···O, O–H···Cl, C–H···π and π–π interactions) within these crystalline chiral enantiomers, forming a stable noncovalent-bonding network

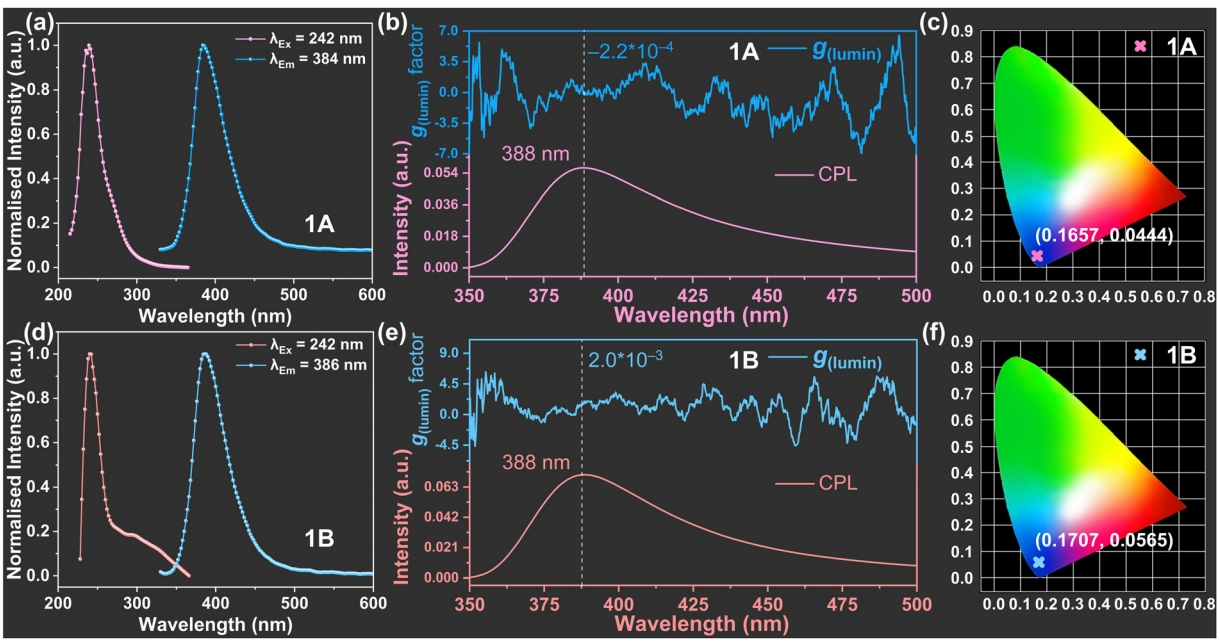

Fig. 2 Excitation and emission spectra (a), circularly polarized luminescence spectra (b) and CIE coordinates (c) of **1A** at room temperature. Excitation and emission spectra (d), circularly polarized luminescence spectra (e) and CIE coordinates (f) of **1B** at room temperature.

(Fig. 1c, Fig. S6 and Tables S2–S6, ESI†). In **1A** and **1B**, π–π stacking between naphthalene rings and electrostatic interactions stabilize the crystal structure, while facilitating charge transfer by enhancing molecular proximity, as evidenced by our photoluminescence data.[19–21] Moreover, the fully occupied lone pair of electrons on the phosphorus atom endows the methylated product with exceptional stability and antioxidant properties, rendering it highly resistant to oxidative reactions. Even after three months of air exposure and subsequent ozone fumigation, its phase and structure remain virtually unchanged, as confirmed by PXRD, Raman, and infrared spectroscopy measurements (Fig. S7–S9, ESI†).

To thoroughly explore the possibility of practical applications of these chiral enantiomers, investigations on the photophysical properties of compounds **1A** and **1B** were conducted at room temperature. As shown in Fig. 2a and d, their fluorescence spectra revealed that both compounds exhibited optimal excitation wavelengths at 242 nm. Upon excitation at 242 nm, compound **1A** emitted most efficiently at 384 nm, while compound **1B** emitted at 386 nm. These results indicate that both compounds are typical blue-light-emitting materials. Additionally, the narrow emission peaks suggest high color purity for both compounds. Compared to non-chiral compounds, chiral compounds not only exhibit conventional photoluminescence (PL) characteristics but also possess chiral luminescence features.[22] To better characterize the chiral luminescence properties of **1A** and **1B**, circularly polarized luminescence (CPL) spectra were measured at room temperature. As shown in Fig. 2b and e, both compounds displayed optimal CPL at 388 nm. At this emission wavelength, the asymmetry factor (g_{lum}) for **1A** was approximately -2.2×10^{-4}, whereas for **1B** it was about 2.0×10^{-3}. This indicates that both compounds exhibit favourable blue-light CPL performance. Internationally, the Commission Internationale de l'Eclairage (CIE) coordinates (CIE_x, CIE_y) are commonly used to describe the luminescence color gamut. Using the CIE 1931, the emission spectra of compounds **1A** and **1B** were calculated and plotted on color gamut diagrams. The data indicated that the color coordinates of the crystalline materials were (0.1657, 0.0444) for **1A** and (0.1707, 0.0565) for **1B** (Fig. 2c and f). According to the National Television System Committee (NTSC) deep blue gamut standard ($CIE_y < 0.08$), both compounds qualify as deep blue gamut photoluminescence materials.[23,24] Compounds **1A** and **1B** exhibit promising potential as commercial circularly polarized blue light materials for application in the high-end display industry.

Molecular electrostatic potential (MESP) topology analysis can directly reveal the fundamental phenomena of through-space effects (TSE) of molecules, which impart donor–acceptor properties to the compounds through steric hindrance.[25] The TSE reflects the extent to which the electron cloud of a molecule interacts across space, a phenomenon that not only governs the reactivity of the molecule but also influences its ability to act as a donor or an acceptor in chemical reactions and coordination processes.[26] The MESP maps of **1A** and **1B** were plotted using the Gaussian 16 package[27] employing the CAM-B3LYP hybrid meta exchange–correlation functional and the def2-TZVP basis set.[28] The electrostatic potential data indicate that regions associated with the organic molecules appear red, signifying higher potential, which suggests that the organophosphate cations are in an electronically diffuse state and carry a positive charge. In contrast, regions containing counterions (Cl^- and H_3O^+) and solvent water molecules appear blue, indicating that these areas have a higher negative charge density (Fig. 3a and c). The MESP of **1A** and **1B** showed very similar features, as expected for enantiomers, with any apparent difference resolved by proper alignment. Besides, the Hirshfeld surface and fingerprint plots can be used to further analyze the types and compositions of non-covalent interactions in the system (Fig. 3b and d). The Hirshfeld surface analysis reveals that both compounds exhibit abundant non-covalent interactions, such as H···C (C–H···π), C···H (π···H–C), H···H, H···O (O–H···O), and H···Cl (O–H···Cl). The fingerprint plots show that the H···C enrichment ratios for **1A** and **1B** are 13.6% and 11.1%, respectively, while the C···H enrichment ratios are approximately 13.6% and 13.7%. These data suggest that both compounds feature abundant van der Waals interactions. Additionally, the H···O enrichment ratios for **1A** and **1B** are approximately 6.8% and 5.9%, respectively, and the H···Cl enrichment ratios are around 7.8% and 8.5%. Weak interactions play a key role in ensuring stability at room temperature. Besides, TG & DSC results demonstrate that these compounds maintain stability up to 200 °C, while the oxidative tests further confirm their durability. These combined properties support the potential applications of these compounds in deep blue luminescence devices.

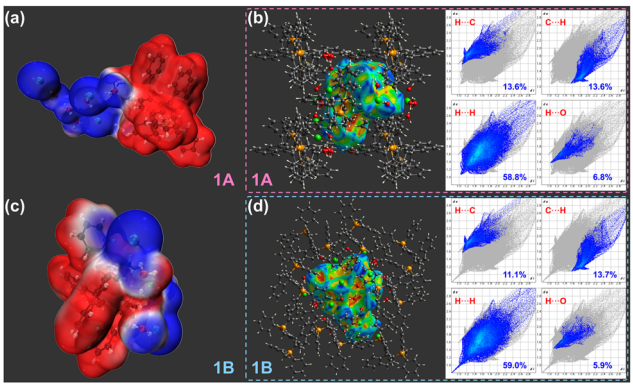

Fig. 3 Electrostatic potential on the van der Waals surfaces of **1A** (a) and **1B** (c). The Hirshfeld surface and 2D fingerprint plots for **1A** (b) and **1B** (d).

The photoluminescence in the organic ammonium salt system is almost entirely attributed to charge transfer within the organic cation.[29,30] To further analyze the charge transfer characteristics of **1A** and **1B**, the band structures and density of states of the cationic parts were calculated using the DMol3 program,[31] and the molecular orbital distributions of the cationic groups were analyzed. Theoretical band structures indicate that both compounds **1A** and **1B** are indirect semiconductors, with theoretical band gaps of 2.709 eV and 2.789 eV, respectively (Fig. 4a and c). The theoretical calculation

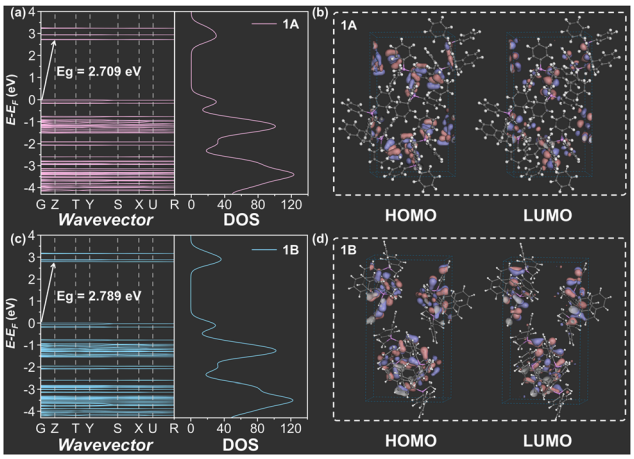

Fig. 4 The calculated band structure and density of states of **1A** (a) and **1B** (c), and their HOMO and LUMO distributions: ((b) for **1A** and (d) for **1B**).

results are in good agreement with those of UV-Vis diffuse reflectance spectroscopy, which supports the accuracy of our calculation model. This further confirms that the luminescence of the compound originates from the charge transfer within the organic phosphonium cations and between the molecules (Fig. S10, ESI†). The relatively wide band gap lays the foundation for the deep blue emission of the materials. Additionally, the electrons in the crystals undergo transitions under light stimulation, manifesting as excited states. In the excited state, electrons dissipate energy in the form of heat through vibrational relaxation, and some electrons also transition back to the ground state, releasing energy in the form of light. Molecular orbital distribution analysis reveals that charge transfer occurs not only within the molecule, from one naphthalene ring to another (LUMO to HOMO), but also between molecules, indicating intermolecular charge transfer (Fig. 4b and d). Moreover, the molecular orbital distributions calculated using the Gaussian 16 package[27] were highly consistent with those of DMol3, further confirming the charge transfer process (Fig. S11, ESI†).

Conclusions

In conclusion, stable blue-emitting enantiomeric crystalline materials were successfully synthesized *via* a facile one-step methylation reaction of phosphine compounds. Compared to their precursor counterparts, these materials not only preserve their highly efficient chiral luminescence properties but also exhibit significantly improved thermal stability and antioxidative performance. Comprehensive spectroscopic analysis and circular polarization measurements further confirm that the methylated products emit deep blue light, characterized by a CIE coordinate *y* value below 0.08. These findings underscore the potential of these materials as commercially viable candidates for circularly polarized luminescent applications in wide-color-gamut OLED displays. This work establishes a theoretical framework for advancing the commercialization of circularly polarized deep-blue-emitting materials.

Author contributions

Si-Fan Lu performed the experiments, data analyses, and manuscript writing; Meng-Na Jing provided suggestions and guidance on structural characterization; Mian-He Xu performed part of the theoretical calculations; Jian Lu performed the theoretical analyses, guided and supervised the experiments, and revised the paper; Fa-Kun Zheng and Guo-Cong Guo offered some advice on manuscript writing. All authors contributed to the general discussion.

Data availability

The data supporting this article have been included as part of the ESI.†

Conflicts of interest

The authors declare that they have no known competing financial interests or personal relationships that could have appeared to influence the work reported in this paper.

Acknowledgements

This work was supported by the National Natural Science Foundation of China (22205237 and 22271283), the Central Leading Local Science and Technology Development Special Project (2021L3025), the Natural Science Foundation of Fujian Province of China (2024J08293) and the Scientific Instrument Developing Project of the Chinese Academy of Sciences (YJKYYQ20210039).

Notes and references

1 Y. Sang, J. Han, T. Zhao, P. Duan and M. Liu, Circularly polarized luminescence in nanoassemblies: generation, amplification, and application, *Adv. Mater.*, 2020, **32**, 1900110.
2 Y. Zhang, S. Yu, B. Han, Y. Zhou, X. Zhang, X. Gao and Z. Tang, Circularly polarized luminescence in chiral materials, *Matter*, 2022, **5**, 837–875.
3 D.-W. Zhang, M. Li and C.-F. Chen, Recent advances in circularly polarized electroluminescence based on organic light-emitting diodes, *Chem. Soc. Rev.*, 2020, **49**, 1331–1343.
4 K. Yang, R. Zhang, Y. Liu, B. Zhao, Y. Wu and J. Deng, Circularly polarized phosphorescence energy transfer combined with chirality-selective absorption for modulating full-color and white circularly polarized long afterglow, *Angew. Chem., Int. Ed.*, 2024, **163**, e202409514.
5 X.-H. Ma, Y. Si, J.-H. Hu, X.-Y. Dong, G. Xie, F. Pan, Y.-L. Wei, S.-Q. Zang and Y. Zhao, High-efficiency pure blue circularly polarized phosphorescence from chiral

N-heterocyclic-carbene-stabilized copper (I) clusters, *J. Am. Chem. Soc.*, 2023, **145**, 25874–25886.
6 X. Deng, F. Zhang, Y. Zhang and H. Shen, Heavy-metal-free blue-emitting ZnSe(Te) quantum dots: synthesis and light-emitting applications, *J. Mater. Chem. C*, 2023, **11**, 14495–14514.
7 X. Wang, Q. Wang, X. Zhang, J. Miao, J. Cheng, T. He, Y. Li, Z. Tang and R. Chen, Circularly polarized light source from self-assembled hybrid nanoarchitecture, *Adv. Opt. Mater.*, 2022, **10**, 2200761.
8 J. Gu, W. Shi, H. Zheng, G. Chen, B. Wei and W.-Y. Wong, The novel organic emitters for high-performance narrow-band deep blue OLEDs, *Top. Curr. Chem.*, 2023, **381**, 26.
9 N. Mehwish, X. Dou, Y. Zhao and C.-L. Feng, Supramolecular fluorescent hydrogelators as bioimaging probes, *Mater. Horiz.*, 2019, **6**, 14–44.
10 G. Suman, M. Pandey and A. J. Chakravarthy, Review on new horizons of aggregation induced emission: from design to development, *Mater. Chem. Front.*, 2021, **5**, 1541–1584.
11 M. Saqlain, H. M. Zohaib, S. Qamar, H. Malik and H. Li, Strategies for the enhancement of CPL properties, *Coord. Chem. Rev.*, 2024, **501**, 215559.
12 J.-C. Blancon, J. Even, C. C. Stoumpos, M. G. Kanatzidis and A. D. Mohite, Semiconductor physics of organic–inorganic 2D halide perovskites, *Nat. Nanotechnol.*, 2020, **15**, 969–985.
13 X. Feng, X. Wang, C. Redshaw and B. Z. Tang, Aggregation behaviour of pyrene-based luminescent materials, from molecular design and optical properties to application, *Chem. Soc. Rev.*, 2023, **52**, 6715–6753.
14 N. Goel, A. Kushwaha, M. Kwoka and M. Kumar, Strategic review of organic–inorganic perovskite photodetectors, *Phys. Status Solidi RRL*, 2024, **18**, 2400110.
15 J. Liu, X. Zhou, X. Tang, Y. Tang, J. Wu, Z. Song, H. Jiang, Y. Ma, B. Li and Y. Lu, Circularly polarized organic ultralong room-temperature phosphorescence: generation, enhancement, and application, *Adv. Funct. Mater.*, 2024, 2414086.
16 X. Cheng and W. Zhang, Polymerization-induced chiral self-assembly for the *in situ* construction, modulation, amplification and applications of asymmetric suprastructures, *Angew. Chem., Int. Ed.*, 2024, **163**, e202414332.
17 J. Lu, R.-X. Qian, S.-F. Lu, S.-H. Wang, F.-K. Zheng and G.-C. Guo, High-resolution X-ray circular polarization Imaging enabled by luminescent photopolymerized chiral metal-organic polymers, *Adv. Funct. Mater.*, 2024, **34**, 2410219.
18 G. Xu, G.-C. Guo, M.-S. Wang, Z.-J. Zhang, W.-T. Chen and J.-S. Huang, Photochromism of a methyl viologen bismuth (III) chloride: structural variation before and after UV irradiation, *Angew. Chem., Int. Ed.*, 2007, **46**, 3249–3251.
19 Y. Hou, X. Zhang, K. Chen, D. Liu, Z. Wang, Q. Liu, J. Zhao and A. Barbon, Charge separation, charge recombination, long-lived charge transfer state formation and intersystem crossing in organic electron donor/acceptor dyads, *J. Mater. Chem. C*, 2019, **7**, 12048–12074.
20 S. I. Bokarev, O. S. Bokareva and O. Kuehn, A theoretical perspective on charge transfer in photocatalysis. The example of Ir-based systems, *Coord. Chem. Rev.*, 2015, **304**, 133–145.
21 J. Lu, H.-F. Wu, W.-F. Wang, J.-G. Xu, F.-K. Zheng and G.-C. Guo, Calcium-based efficient cathode-ray scintillating metal–organic frameworks constructed from π-conjugated luminescent motifs, *Chem. Commun.*, 2019, **55**, 13816–13819.
22 F. Pop, N. Zigon and N. Avarvari, Main-group-based electro- and photoactive chiral materials, *Chem. Rev.*, 2019, **119**, 8435–8478.
23 M. Derbel and A. Mbarek, Optical properties and stability of a blue-emitting phosphor Sr2P2O7: Eu2+ under UV and VUV excitation, *Mech. Eng. Technol. Appl.*, 2021, **1**, 72–86.
24 R. Korpe, K. Koparkar, N. Bajaj and S. Omanwar, VUV investigation of blue emitting MAl12O19: Eu (M = Ca, Sr, Ba) phosphors synthesized by combustion method, *J. Phys.:Conf. Ser.*, 2020, **1**, 012056.
25 J. S. Murray and P. Politzer, The electrostatic potential: an overview, *Wiley Interdiscip. Rev.: Comput. Mol. Sci.*, 2011, **1**, 153–163.
26 S. E. Wheeler and K. N. Houk, Through-space effects of substituents dominate molecular electrostatic potentials of substituted arenes, *J. Chem. Theory Comput.*, 2009, **5**, 2301–2312.
27 M. J. Frisch, G. W. Trucks, H. B. Schlegel, G. E. Scuseria, M. A. Robb, J. R. Cheeseman, G. Scalmani, V. Barone, G. A. Petersson, H. Nakatsuji, X. Li, M. Caricato, A. V. Marenich, J. Bloino, B. G. Janesko, R. Gomperts, B. Mennucci, H. P. Hratchian, J. V. Ortiz, A. F. Izmaylov, J. L. Sonnenberg, D. Williams-Young, F. Ding, F. Lipparini, F. Egidi, J. Goings, B. Peng, A. Petrone, T. Henderson, D. Ranasinghe, V. G. Zakrzewski, J. Gao, N. Rega, G. Zheng, W. Liang, M. Hada, M. Ehara, K. Toyota, R. Fukuda, J. Hasegawa, M. Ishida, T. Nakajima, Y. Honda, O. Kitao, H. Nakai, T. Vreven, K. Throssell, J. A. Montgomery, Jr., J. E. Peralta, F. Ogliaro, M. J. Bearpark, J. J. Heyd, E. N. Brothers, K. N. Kudin, V. N. Staroverov, T. A. Keith, R. Kobayashi, J. Normand, K. Raghavachari, A. P. Rendell, J. C. Burant, S. S. Iyengar, J. Tomasi, M. Cossi, J. M. Millam, M. Klene, C. Adamo, R. Cammi, J. W. Ochterski, R. L. Martin, K. Morokuma, O. Farkas, J. B. Foresman and D. J. Fox, *Gaussian 16, Rev. C.01*, 2016.
28 T. Yanai, D. P. Tew and N. C. Handy, A new hybrid exchange-correlation functional using the Coulomb-attenuating method (CAM-B3LYP), *Chem. Phys. Lett.*, 2004, **393**, 51–57.
29 S. L. De Rooy, B. El-Zahab, M. Li, S. Das, E. Broering, L. Chandler and I. M. Warner, Fluorescent one-dimensional nanostructures from a group of uniform materials based on organic salts, *Chem. Commun.*, 2011, **47**, 8916–8918.
30 G. Xing, D. Peng and T. Ben, Crystalline porous organic salts, *Chem. Soc. Rev.*, 2024, **53**, 1495–1513.
31 B. Delley, From molecules to solids with the DMol3 approach, *J. Chem. Phys.*, 2000, **113**, 7756–7764.